THE JOURNAL OF PHYSICAL CHEMISTRY A

ARTICLE

pubs.acs.org/JPCA

Structure of Co-Doped Alq_3 Thin Films Investigated by Grazing Incidence X-ray Absorption Fine Structure and Fourier Transform Infrared Spectroscopy

Liang Lin,[†] Zhiyong Pang,[†] Shaojie Fang,[†] Fenggong Wang,[†] Shumei Song,[‡] Yuying Huang,[§] Xiangjun Wei,[§] Haisheng Yu,[§] and Shenghao Han*[,†,‡]

[†]School of Physics, State Key Laboratory of Crystal Materials, Shandong University, Jinan 250100, P. R. China

[‡]School of Space Science and Physics, Shandong University at Weihai, Weihai 264209, P. R. China

[§]Shanghai Institute of Applied Physics, Chinese Academy of Sciences, Shanghai 201204, P. R. China

ABSTRACT: The structural properties of Co-doped tris-(8-hydroxyquinoline)aluminum (Alq_3) have been studied by grazing incidence X-ray absorption fine structure (GIXAFS) and Fourier transform infrared spectroscopy (FTIR). GIXAFS analysis suggests that there are multivalent Co-Alq_3 complexes and the doped Co atoms tend to locate at the attraction center with respect to N and O atoms and bond with them. The FTIR spectra indicate that the Co atoms interact with the meridional (*mer*) isomer of Alq_3 rather than forming inorganic compounds.

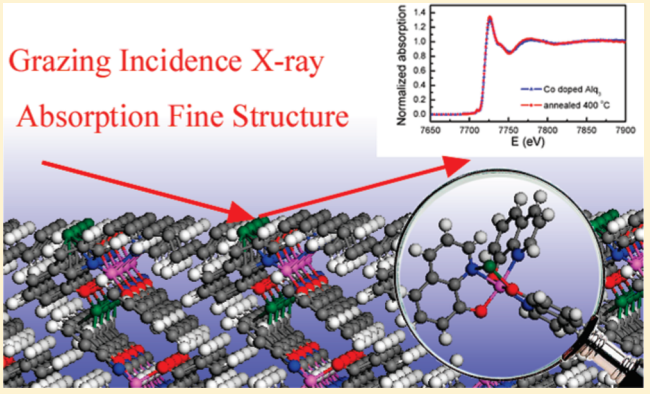

INTRODUCTION

The π-conjugated molecular semiconductor tris(8-hydroxyquinoline)aluminum (Alq_3, $C_{27}H_{18}N_3O_3Al$) has been widely used as electron transporting and light-emitting material in organic light-emitting devices (OLEDs) by virtue of its high electroluminescence (EL) efficiency.[1] Recently, Baik et al. reported ferromagnetism in 3d transition metal (Mn, Ni, and Co) doped Alq_3 thin films synthesized by thermal coevaporation of pure Co (Mn, Ni) and Alq_3 powders.[2,3] However, the detailed mechanism still remains unknown. It is well-known that the magnetism is strongly related to the molecule structure. In our previous theoretical work,[4] it is found that the Co atoms tend to interact with the Alq_3 molecules with some electron density transferred from Co atoms to the molecule. And the attraction centers of phenoxide rings, N and O atoms and two O atoms are possible Co locations. However, corresponding experimental investigation are needed.

In this work, the structural properties of Co-doped Alq_3 are studied by grazing incidence X-ray absorption fine structure (GIXAFS) and Fourier transform infrared spectroscopy (FTIR). The X-ray absorption fine structure (XAFS) measurements at the *K* edge are very helpful for determining the valence state and local structure of Co element in Co doped oxide systems. It can detect the Co element even if they are disordered or in the form of small nanoparticles. GIXAFS has an advantage over normal XAFS since there is no strict requirement on thickness of the measured films. The vibrational analysis of the Fourier transform infrared spectroscopy (FTIR) is a conventional method to differentiate the different symmetries of isomers of Alq_3. In combination with ab initio calculations,[5,6] the FTIR can infer the structures of the components by virtue of the functional group information.

EXPERIMENTAL METHODS

The Si substrate was loaded into a thermal evaporator at 1.5×10^{-4} Pa, on which Co-doped Alq_3 film with a thickness of 120 nm was prepared by coevaporating pure Co metal (99.99%) and Alq_3 powders (99.995%) at room temperature. The Co concentration in Alq_3 film was 4 wt % (Co/Al atomic ratio = 0.3) by different evaporating rates of Co and Alq_3. The film thickness was in situ monitored by a quartz crystal thickness monitor, and the deposition rate was confirmed by the thickness profilometer. Then, the sample was divided into two segments with the same size (10 mm × 10 mm). One of them was annealed at 400 ± 5 °C in a 5×10^{-4} Pa chamber for 1 h, at a heating rate of 10 °C min^{-1} and natural cooling.

Thermal analysis was performed by differential scanning calorimertry (DSC) using a CDR-4P. Samples (~16 mg) of

Received: October 8, 2010
Revised: December 13, 2010
Published: January 7, 2011

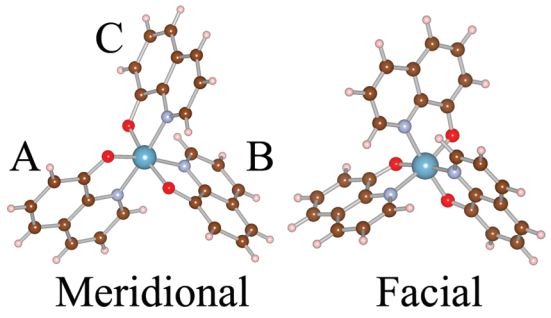

Figure 1. Meridional (*mer*) and facial (*fac*) isomers of Alq_3. The A, B, and C labels of the three quinoline ligands are identical to those used in the study of the vibrational modes of Alq_3. The darker blue, red, lighter blue, brown, and pink balls represent aluminum, oxygen, nitrogen, carbon, and hydrogen atoms, respectively.

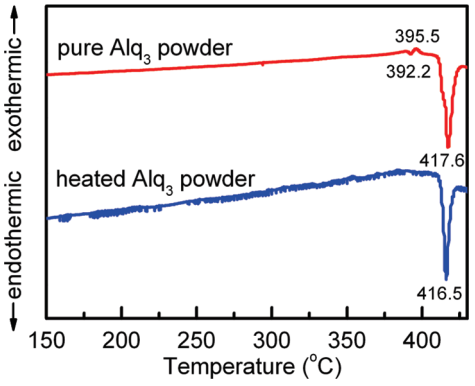

Figure 2. DSC curves of pre- and postevaporated Alq_3 powders taken with a heating rate of 10 °C min^{-1}, respectively.

pre- and postevaporated Alq_3 powders were placed in aluminum pans and heated at a rate of 10 °C/min^{-1}. XAFS experiments were carried out at the XAFS station of the Shanghai Synchrotron Radiation Facility (SSRF). The beamline provided a focused X-ray beam from 4 to 22.5 keV with a photon flux on the order of 10^{13} phs/s (@ 10 keV) and a beam size of 0.2 mm × 0.3 mm. The energy was calibrated by a standard Co metal foil before experiments started. Co *K*-edge GIXAFS spectra of the samples were collected by a silicon drift detector. Because the samples were amorphous organic based materials, the signal-to-noise ratio was poor at the extended X-ray absorption fine structure (EXAFS) part. So, the X-ray absorption near-edge structure (XANES) was collected from −150 to +180 eV relative to the Co *K*-edge. The data analysis of XANES was carried out using the Athena and Artemis interfaces to the IFEFFIT program package.[7] FTIR spectra were recorded in the 400−4000 cm^{-1} region on the VERTEX-70 spectrometer with 1−4 cm^{-1} resolution. All the films were prepared on the KBr substrates, which were transparent in infrared spectroscopy, with the same condition as that on the Si substrates.

RESULTS AND DISCUSSION

To understand the structural properties of Co-doped Alq_3, the symmetries of isomers must be determined first. Four crystalline phases α, *β*, *γ*, and *δ* of Alq_3 have been identified. The α- and *β*-phases are low-temperature phases with meridional (*mer*) isomers, and the *γ*- and *δ*-phases are high-temperature phases with facial (*fac*) isomers. Generally, Alq_3 molecules adopt *mer*-Alq_3

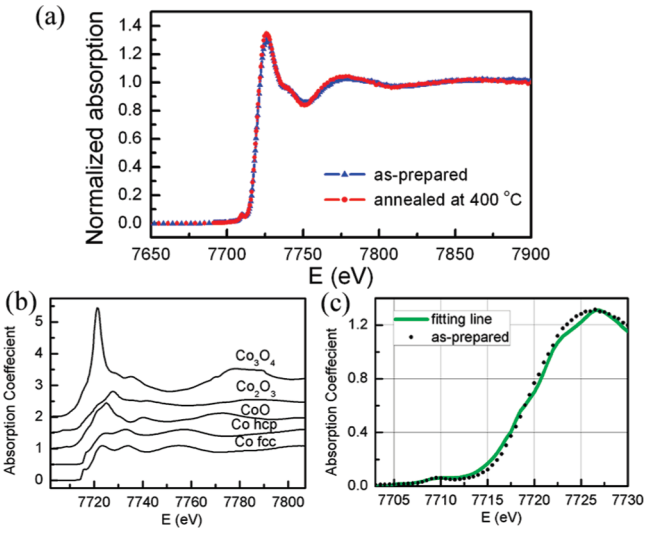

Figure 3. (a) Co *K*-edge XANES spectra of as-prepared Co-doped Alq_3 films and films annealed at 400 °C, respectively. (b) Co *K*-edge XANES standard spectra of Co metal and Co oxide, respectively. (c) Examples of the near-edge fitting for the Co-doped Alq_3, with a significant peak of the Co oxide. The points are the measured data, and the fit using *fcc* Co, Co_2O_3, and CoO for are compared. The fitting range was 7700−7730 eV.

isomeric form with C_1 symmetry in both solution and solid state, and *fac*-Alq_3 with C_3 symmetry could only been obtained by annealing *mer*-Alq_3 solid at a high temperature (Figure 1). Although density functional theory (DFT) calculations have predicted that the metal−Alq_3 (*fac*) complexes are more stable than metal−Alq_3 (*mer*) complexes and *fac*-Alq_3 adsorbed on Co surface has been studied by photoemission experiments,[8,9] *mer*-Alq_3 complexes have been admitted in most papers.[2−4,10,11] Figure 2 shows the DSC curves of the pre- and postevaporated Alq_3 powders taken with a heating rate of 10 °C min^{-1}, respectively. The pre-evaporated one was observed with a coupled endothermic and exothermic phase transition at about 392 °C, prior to the melting transition at 417 °C. This phase transition at 392 °C had also been reported before and attributed to the phase transition from the α-phase to the *γ*-phase.[12] Generally, the high temperature phase would transform to the low temperature phase as the powder cools to room temperature. However, the phase transition at 392 °C did not appear in the postevaporated Alq_3 powder, indicating that the postevaporated Alq_3 powders were not of the same phase as the pre-evaporated one; it should be *β*-phase. This is because the *β*-phase of Alq_3 is a stable phase and no transition regarding the *β*-phase has been reported to date.

Figure 3a shows the normalized Co *K*-edge XANES spectra of as-prepared Co-doped Alq_3 films and films annealed at 400 °C, respectively. The spectra show main features of XANES spectra with a small pre-edge peak and a dominant main peak. The interpretations of *K*-edge XANES features for 3d transition-metal oxides are well established. Generally, the small pre-edge peak is interpreted as a quadrupolar electronic transition from 1s to the 3d final states hybridized with 4p character of the absorber. Its intensity is enhanced by the local atomic configuration that lacks centrosymmetry.[13,14] The dominant main peak arises from the dominant dipolar transition from 1s to the 4p-related final states. Thus, the small pre-edge peak at 7709.4 eV can be considered as the fingerprint peak of the bonds between Co

dx.doi.org/10.1021/jp109651u |*J. Phys. Chem. A* 2011, 115, 880–883

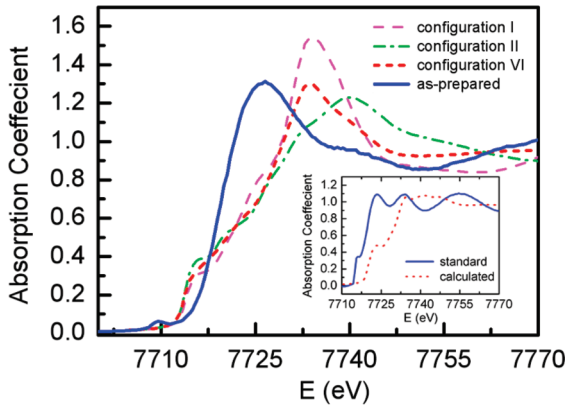

Figure 4. Co K-edge XANES spectra of the as-prepared Co-doped Alq_3 films and theoretical spectra of different Co-Alq_3 configurations calculated using FEFF8. The Co-Alq_3 configurations are optimized Co-doped Alq_3 crystal taken from ref 4.

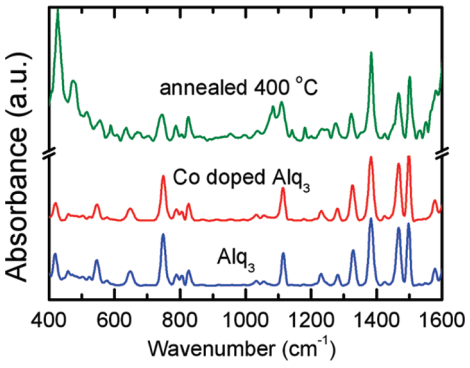

Figure 5. FTIR spectra of the pure Alq_3 film, the as-prepared Co-doped Alq_3 film, and Co-doped Alq_3 film annealed at 400 °C, respectively. These films were deposited onto KBr substrates.

atoms and neighbor nonmetal atoms (i.e., O, N, and C) in the samples. [14] Combined with the observation of XANES spectra at O *K*-edge,[3] Co−O bonds have a significant contribution to this pre-edge peak. Compared with the standard spectra of metal cobalt and cobalt oxides in Figure 3b, the absorption edge at 7720 eV and the maximum height of the main peak at 1.36 indicate a Co(2+) valence in the Co-doped Alq_3 samples. The high-energy (above 7780 eV) atomic absorption spectra, which is due to the core transitions form 1s to 4p states and often show wave line in inorganic compounds, is very smooth, indicating that the Co atoms interact with the Alq_3 molecule rather than forming inorganic compounds.[15]

For a further investigation of the valences and components of the Co-doped Alq_3 films, linear XANES curve fitting were performed. Unfortunately, XANES investigations of Co-organic complexes are rather rare and no related standard spectra can be found to fit. Substitutingly, the standard spectra of metal cobalt and cobalt oxides are used to explore the valences of the Co-doped Alq_3. The fittings were carried out for the lower half of the edge, which is more sensitive to the valences. The structure of Co metal should be taken into account since Co metal with either hexagonal-closed packed (hcp) or face-centered cubic (fcc) structures might form during the coevaporating process. The approach is to fit the near edge with a linear combination of the standard spectra of metal cobalt and cobalt oxides. Figure 3c shows the fitting result of the Co-doped Alq_3 sample, in which the percentage of Co(0) valence (fcc), Co(2+) valence, and Co(3+) valence are about 10%, 70%, and 20%, respectively. Co(2+) is the main component of the Co-Alq_3 complexes.

The components of the Co-doped Alq_3 have been investigated by ab initio multiple scattering cluster calculations on the Co *K*-edge XANES using FEFF8 calculation program.[16] Three possible configurations obtained using DFT calculation in our previous work are chosen.[4] For configuration I, one Co atom locates at the attraction center with respect to N and O atoms while the other Co atom locates near the attraction center of the pyridyl ring of the same molecule. For configuration II, both Co atoms locate at the attraction center sites with respect to N and O atoms but in different molecules. For configuration VI, both Co atoms locate at the attraction center sites with respect to N and O atoms in the same molecule. The calculated results are shown in Figure 4, and the inset shows the calculated curve and standard spectra of Co (fcc), respectively. Although there is a difference between the amorphous samples and the single crystalline configuration for calculation, the calculated Co *K*-edge XANES curve of configurations I and VI are quite consistent with the experimental observation, suggesting that the doped Co atoms tend to locate at the attraction center with respect to N and O atoms and bond with them. In this case, the Co 3d electrons are hybridization with 2p states of O and N atoms, and the outer electronic configuration of Co change from $3d^74s^2$ to $3d^54s^2$. The crystal field splits the degenerate d orbital to five nondegenerate orbitals, each of which can be occupied by two electrons with opposite spins. The majority impurity states are almost fully occupied, while the minority impurity states are only partially occupied, leading electron transferred to the 2p states of nonmetal atoms. Thus, the different occupation of the majority and minority Co d orbitals leads to net local magnetic moment.

The XANES spectra have been also investigated at O *K*-edge by the total-electron-yield (TEY) mode. The spectra suggest that one new peak due to the chemical reaction emerged and the doped Co atoms weaken the structure corresponding to transitions from the 1s orbital to the low unoccupied molecular orbital, which are consistent with Baik et al.'s observation.[3]

Figure 5 shows the FTIR spectra of the pure Alq_3 film, the as-prepared Co-doped Alq_3 film, and Co-doped Alq_3 film annealed at 400 °C, respectively. The FTIR spectra further confirm the *mer*-isomers. Although most vibrational modes of the A, B, and C ligands (labeled in Figure 1) in *mer*-Alq_3 are found to be coupled to one another, the pyramidalization modes O_{CCC} and the angle bending modes δ_{CCC} may be expected to be distinct for all three (A, B, and C) quinolinate fragments in the *mer*-isomer and give rise to splitting peaks at about 824 and 790 cm^{-1}, respectively.[17] In the fingerprint region 720−850 cm^{-1}, the splitting peaks that appear clearly at 788 and 805 cm^{-1} correspond to $\delta_{CCC}{}^{A}$ and $\delta_{CCC}{}^{C}$, respectively, indicating the existence of the *mer*-isomer in this crystal structure. This result is consistent with the anticipation from the DSC measurement.

The FTIR peak intensities and positions of Alq_3 film in the range 750−1600 cm^{-1}, in which the vibrational modes of the quinolinate ligands are mainly included, highly resemble those of Co-doped Alq_3. This proves that the doped Co atoms do not locate at the sites near the phenoxide ring attraction center or bond with C atoms. At frequencies below 700 cm^{-1}, these modes are the characteristics for the vibrations of the metal (Al) with the heteroatoms. The effect of the interaction forces among A, B, and C ligands is to push the system toward a better synchronization

Table 1. Comparison of FTIR Frequencies (cm^{-1}) among the Pure Alq_3 Powders (Ref 6), the Pure Alq_3 Film, the As-Prepared Co-Doped Alq_3 Film, and the Co-Doped Alq_3 Film Annealed at 400 °C between 400 and 700 cm^{-1} [a]

mode	Alq_3 (ref 6)	Alq_3	as-prepared	annealed at 400 °C
$\delta COAl^A$, $\delta COAl^C$	403	399	400	409
$\delta COAl^B$, νOAl^A	418	419	420	426
$\mathcal{O}N^C$, $\mathcal{O}N^A$	458	459	459	472
νOAl^A, δCCC^B	523	523	523	517
νOAl^A	544	545	546	556
$\delta COAl^A$, δCCC^A	575	576	576	588
$\mathcal{O}N^C$, $\mathcal{O}C^A$	649	648	648	636
				669

[a] The column "mode" is the local oscillators giving rise to the larger contributions to the normal modes, where ν, δ, $\mathcal{O}$, A, B, C refer to the bond stretching, the angel bending, the pyramidalization, the A quinolinato, the B quinolinato, and the C quinolinato, respectively.

of the vibrational modes of the fragments and is characteristic of the organometallic complexes.[5] In our case, the doped Co atoms are considered to interact with O atoms of the ligands, which bring about changes in the vibrational modes in the region below 700 cm^{-1}. In fact, only the sample annealed at 400 °C shows small absorption peak intensity and weak offset of frequency between 400 and 700 cm^{-1}. The detailed positions of peaks are shown in Table 1. The decrease of absorption peak intensity indicates that the thickness of the sample is decreased after annealing at 400 °C as a result of sublimation of the Alq_3. In the as-prepared Co-doped Alq_3 sample, the Alq_3 coexist with the Co−Alq_3 complexes and is the major constituent of the sample. The FTIR spectra of as-prepared Co-doped Alq_3 sample show the characteristic peaks of the Alq_3, with peaks of the Co−Alq_3 complexes being negligible. Moreover, the offsets of frequency between 400 and 700 cm^{-1} suggest that the doped Co have an effect on the distance of Al−O bonds and the angles of Al−O−C, resulting in the changes of the bond stretching mode ν and the angle bending modes δ. In fact, the new peak at 669 cm^{-1} is suspected to be caused by the stretching vibration of Co−O bonds. Therefore, the FTIR of the sample annealed at 400 °C show the real vibrational modes of the Co−Alq_3 complexes.

CONCLUSIONS

In summary, we have investigated the structure of coevaporated Co-doped Alq_3 using GIXAFS and FTIR. Co-Alq_3 complexes are constituted of doped Co and *mer*-Alq_3, where the Co ions chemically interact with the O on the quinolinato during the coevaporation. The as-prepared sample may contain Alq_3 and Co-Alq_3 complexes with multivalences. The Co(2+) valence is the main valence of the Co-Alq_3 complexes. The doped Co atoms tend to locate at the attraction center of N and O atoms. After annealing at 400 °C, the new compound with Co-Alq_3 complexes show better thermal stability than that of the Alq_3 films.

AUTHOR INFORMATION

Corresponding Author

*Tel: +86-531-88365435. Fax: +86-531-88365435 E-mail: hansh@sdu.edu.cn.

ACKNOWLEDGMENT

We thank SSRF in Shanghai for use of synchrotron radiation facilities, and Dr. Yonghua Du at National University of Singapore for helpful discussions. We are grateful for financial support from the Natural Science Foundation of China (Grant No. 10974118), Shandong Province Natural Science Foundation (ZR2009GQ010), the Scientific Technological Developing Scheme of Shandong Province (Grant No. 2008GG30004004), and the Independent Innovation Foundation of Shandong University (IIFSDU, 2010TS056).

REFERENCES

(1) Tang, C. W.; VanSlyke, S. A. *Appl. Phys. Lett.* **1987**, *51*, 913–915.
(2) Baik, J. M.; Lee, J.-L.; Shon, Y.; Kang, T. W. *Phys. Status Solidi* **2008**, *2*, 22–24.
(3) Baik, J. M.; Shon, Y.; Lee, S. J.; Jeong, Y. H.; Kang, T. Won; Lee, J. L. *J. Am. Chem. Soc.* **2008**, *130*, 13522–13523.
(4) Wang, F.; Pang, Z.; Lin, L.; Fang, S.; Dai, Y.; Han., S. *Appl. Phys. Lett.* **2010**, *96*, 053304.
(5) Esposti, A. D.; Brinkmann, M.; Ruani, G.; Zamboni, R. *Synth. Met.* **2002**, *127*, 247–250.
(6) Esposti, A. D.; Brinkmann, M.; Ruani, G. *J. Chem. Phys.* **2002**, *116*, 798–813.
(7) Ravel, B.; Newville, M. *J. Synchrotron Radiat.* **2005**, *12*, 537–541.
(8) Curioni, A.; Andreoni, W. *J. Am. Chem. Soc.* **1999**, *121*, 8216–8220.
(9) Caruso, A. N.; Schulz, D. L.; Dowben, P. A. *Chem. Phys. Lett.* **2005**, *413*, 321–325.
(10) Brinkmann, M.; Gadret, G.; Muccini, M.; Taliani, C.; Masciocchi, N.; Sironi, A. *J. Am. Chem. Soc.* **2000**, *122*, 5147–5157.
(11) Parthasarathy, G.; Shen, C.; Kahn, A.; Forrest, S. R. *J. Appl. Phys.* **2001**, *89* (9), 4986–4992.
(12) Sapochak, L. S.; Padmaperuma, A.; Washton, N.; Endrino, F.; Schmett, G. T.; Marshall, J.; Fogarty, D.; Burrows, P. E.; Forrest, S. R. *J. Am. Chem. Soc.* **2001**, *123*, 6300–6307.
(13) Heald, S. M.; Kaspar, T.; Droubay, T.; Shutthanandan, V.; Chambers, S. *Phys. Rev. B* **2009**, *79*, 075202.
(14) Westre, T. E.; Kennepohl, P.; Dewitt, J. G.; Hedman, B.; Hodgson, K. O.; Solomon, E. I. *J. Am. Chem. Soc.* **1997**, *119* (27), 6297–6314.
(15) Bianconi, A.; Dell'Ariccia, M.; Durham, P. J.; Pendery, J. B. *Phys. Rev. B* **1982**, *26*, 6502–6508.
(16) Ankudinov, A. L.; Bouldin, C. E.; Rehr, J. J.; Sims, J.; Hung, H. *Phys. Rev. B* **2002**, *65*, 104107.
(17) Brinkmann, M.; Fite, B.; Pratontep, S.; Chaumont, C. *Chem. Mater.* **2004**, *16*, 4627–4633.